Dalton Transactions



PAPER



Cite this: *Dalton Trans.*, 2022, **51**, 9103

Synthesis of diphenyl-(2-thienyl)phosphine, its chalcogenide derivatives and a series of novel complexes of lanthanide nitrates and triflates†

Troy Luster,^a Hannah J. Van de Roovaart,^a Kyle J. Korman,^a Georgia G. Sands,^a Kylie M. Dunn,^a Anthony Spyker,^a Richard J. Staples, ^b Shannon M. Biros ^a and John E. Bender *

A novel synthesis of diphenyl(2-thienyl)phosphine, along with its' oxide, sulfide and selenide derivatives, is reported here. These phosphines have been characterized by NMR, IR, MS and X-Ray crystallography. The phosphine oxide derivative was reacted with a selection of lanthanide(III) nitrates and triflates, LnX₃, to give the resultant metal-ligand complexes. These complexes have also been characterized by NMR, IR, MS and X-Ray crystallography. Single crystal X-Ray diffraction data shows a difference in metal-ligand complex stoichiometry and stereochemistry depending on the counteranion (nitrate vs. triflate). The [Ln (Ar₃P=O)₃(NO₃)₃] ligand-nitrate complexes are nine-coordinate to the metal in the solid state (bidentate nitrate), featuring a 1:3 lanthanide-ligand ratio and bear an overall octahedral arrangement of the six, coordinated ligands. Our [Ln(Ar₃P=O)₃(NO₃)₃] ligand-nitrate complexes gave three examples of *fac*-stereochemistry, where *mer*-stereochemistry is almost universally observed in the literature of highly related [Ln (Ar₃P=O)₃(NO₃)₃] complexes. For the Tb complexes, two different arrangements of the ligands around the metal were observed in the solid state for [Tb(Ar₃P=O)₃(NO₃)₃] and [Tb(Ar₃P=O)₄(OTf)₂] [OTf]. [Tb (Ar₃P=O)₃(NO₃)₃] is strictly nine-coordinate, ligand *mer*-stereochemistry in the solid state, and [Tb (Ar₃P=O)₄(OTf)₂] [OTf] is strictly octahedral, six-coordinate, with a square-planar stereochemical arrangement of the phosphine oxide ligands around the metal.

Received 19th May 2022, Accepted 27th May 2022 DOI: 10.1039/d2dt01570f

rsc.li/dalton

Introduction

The elements within the f-block of the periodic table have rich chemical properties that include: the ability to luminescence, to give off energy *via* nuclear decay, and to affect the relaxation of bound water molecules.¹ The exploitation of these properties have made f-block elements components in bioprobes,²⁻⁴ magnets⁵ and LEDs,⁶⁻⁸ a source of alternative

energy,9 and the active ingredient in MRI contrast agents.10 Due to the incorporation of lanthanide metals in many everyday materials, the US Department of Energy has deemed several of these elements as "critical" and has invested millions of dollars 12 into research that will enhance the technology used to isolate these metals from ground ores and end-of-life technologies. Currently, lanthanide (Ln) and actinide (An) metals are most often purified using solvent-solvent extraction methods that utilize a ligand in an organic solvent which extracts the metal out of acidic water. Many of the organic ligands contain a carbonyl, phosphine oxide or phosphine sulfide group which uses its oxygen or sulfur atom(s) to chelate the metal. Hence, the development of new organic ligands with these donor atoms will add to the growing body of knowledge of f-block coordination chemistry and may lead to the development of new compounds for f-element separations.

Triphenylphosphine has a deep, extensively productive history in the chemistry of the transition-metals, 13 but is largely inert to coordination with the Ln(III) metals. Given well known trends in the "hard–soft" paradigm for coordination chemistry, 14 published studies with Ln(III) metals and

^aDepartment of Chemistry, Grand Valley State University, Allendale, MI 49401, USA. E-mail: benderj@gysu.edu

^bCenter for Crystallographic Research, Department of Chemistry, Michigan State University, 578 S. Shaw Lane, East Lansing, MI 48824, USA

[†]Electronic supplementary information (ESI) available: NMR spectra (¹H, ¹³C, ³¹P) for all compounds reported here. X-Ray crystal diffraction data (as .cif files) have been deposited with the Cambridge Structural DatabaseComplete tables, experimental details, figures of each structures showing the thermal ellipsoids and atom numbering scheme, and detailed description of the treatment of any disordered electron density. CCDC 1844568, 1844765, 1846830, 1850479, 1922657, 1922734, 2096359, 2173564 and 2173657. For ESI and crystallographic data in CIF or other electronic format see DOI: https://doi.org/10.1039/d2dt01570f

Fig. 1 Structural types of (left) triphenylphosphine oxide and (right) the diphenyl(2-thienyl) phosphine derivatives discussed in this paper.

commercially available compounds have described stable complexes with the oxides of trialkyl- and triarylphosphines.¹⁵⁻²¹ This is in contrast to the phosphine sulfides and selenides, which are better suited for binding to the softer actinide metals.²² In this work we aimed to develop the synthesis of an unsymmetrical triarylphosphine ligand, where one of the aromatic rings contained a heteroatom that could potentially interact with the Ln or An metal (Fig. 1). The ability to isolate the phosphine will then allow for the straightforward synthesis of three chalcogenide derivatives (oxide, sulfide, selenide). In this report we describe a novel synthesis and characterization of diphenyl(2-thienyl)phosphine along with the oxide, sulfide and selenide. Also described here is a novel series of lanthanide complexes of diphenyl(2-thienyl)phosphine oxide, with unexpected stereochemical outcomes.

Experimental

General considerations

All chemicals (including deuterated solvents) were purchased from Sigma-Aldrich or Strem Chemical and used without further purification. NMR spectral data (1 H, 13 C, 31 P, 77 Se) were recorded on either a JEOL Eclipse 300, Varian Inova 400, or JEOL ECZS 400 NMR spectrophotometer, as stated. For NMR spectra, chemical shifts are expressed as parts per million (δ) relative to SiMe₄ (TMS, δ = 0) for 1 H and 13 C data, H₃PO₄ (δ = 0) for 31 P data and (CH₃)₂Se (δ = 0) for 77 Se data. IR spectra were acquired neat on a Jasco 4100 FTIR. Elemental (CHN) analyses were performed by Atlantic Microlab Inc., Norcross, GA; all CHN percentages calculated for lanthanide complexes assume three phosphine oxide ligands + Ln(NO₃)₃ or Ln(OTf)₃ + residual water/solvents as indicated. Low resolution mass spectrometry data were acquired on a Advion Expression-L Compact Mass Spectrometer.

Single crystal X-ray crystallography

Crystals suitable for X-ray diffraction were mounted on a nylon loop using a small amount of paratone oil. Data were collected using either a Bruker CCD (charge coupled device) or Rigaku OD diffractometer equipped with a low-temperature apparatus operating at 173(2) K. Data were measured using omega and phi scans of 0.5° per frame. The total number of images was based on results from the program COSMO²³ or CrysAlisPro²⁴ where redundancy was expected to be 4.0 and completeness of 100% out to 0.83 Å. Cell parameters were retrieved using either APEX II²⁵ or CrysAlisPro software and refined using SAINT²⁶ or

CrysAlisPro on all observed reflections. Data reduction was performed using the SAINT or CrysAlisPro software, which corrects for Lorentz polarization. Scaling and absorption corrections were applied using either the SADABS²⁷ multi-scan technique, supplied by George Sheldrick, or as implemented in SCALE3 ABSPACK scaling algorithm. The structures were solved using the SHELXS-97 program and refined by least squares method on F^2 , SHELXL-2014, ²⁸ which are incorporated in OLEX2.^{29,30} All non-hydrogen atoms are refined anisotropically. Hydrogen atoms were calculated by geometrical methods and refined as a riding model. The crystals used for the diffraction study showed no decomposition during data collection. Further crystallographic data and experimental details for structural analysis of all of the compounds are summarized in Tables 1 and 3, and selected bond lengths and angles with their estimated standard deviations are given in Tables 2, 4 and 5. Complete tables for each structure reported here, diagrams depicting the thermal ellipsoids, and descriptions of how any disordered electron density was treated are provided in the ESI.†

Table 1 Crystal data and structure refinement information for oxide 4, sulfide 5 and selenide 6

Structure	4	5	6
CCDC number	2096359	1844568	1844765
Empirical formula	$C_{16}H_{13}OPS$	$C_{16}H_{13}PS_2$	$C_{16}H_{13}PSSe$
Formula weight	284.29	300.35	347.25
Temperature/K	99.98(13)	296(2)	173(2)
Crystal system	Monoclinic	Monoclinic	Monoclinic
Space group	$P2_1/n$	$P2_1/n$	$P2_1/n$
a/Å	9.6867(2)	10.18080(10)	10.398(3)
$b/ m \AA$	9.9115(2)	9.50350(10)	9.531(3)
c/Å	14.6285(3)	14.9030(2)	14.811(5)
<i>α</i> /°	90	90	90
β/°	96.773(2)	94.0376(5)	93.489(4)
γ/°	90	90	90
Volume/Å ³	1394.67(5)	1438.33(3)	1465.2(8)
Z	4	4	4
Reflections collected	10173	17 457	11 733
Independent	2697 $R_{int} =$	2831 [$R_{int} =$	2683 [$R_{int} =$
reflections	$0.0393, R_{\text{sigma}} = 0.0359$	$0.0344, R_{\text{sigma}} = 0.0237$	$0.0445, R_{\text{sigma}} = 0.0386$
Final R indexes	$R_1 = 0.0713$,	$R_1 = 0.0548,$	$R_1 = 0.0465$
$[I \ge 2\sigma(I)]$	$wR_2 = 0.1953$	$wR_2 = 0.1545$	$wR_2 = 0.1233$
Final R indexes	$R_1 = 0.0761$,	$R_1 = 0.0569$	$R_1 = 0.0607$
[all data]	$wR_2 = 0.2002$	$wR_2 = 0.1564$	$wR_2 = 0.1324$

Table 2 Selected bond lengths (Å) and angles (°) for oxide 4, sulfide 5 and selenide 6

	4 (X=O)	5 (X=S)	6 (X=Se)
P1-X1	1.514(3)	1.9573(11)	2.1132(12)
P1-C1(thienyl)	1.776(3)	1.792(3)	1.799(4)
P1-C5	1.803(2)	1.812(3)	1.815(4)
P1-C11	1.802(4)	1.813(3)	1.821(4)
X1-P1-C1	112.73(17)	113.01(10)	112.86(14)
X1-P1-C5	111.64(14)	113.38(10)	113.33(13)
X1-P1-C11	112.46(17)	112.66(10)	112.38(14)

Synthesis

Diphenyl(2-thienyl)phosphine 3. A round bottom flask was charged with ca. 25 mL of anhydrous diethyl ether and 550 mg solid Mg turnings. To this solution was added 2.81 g of 2-bromothiophene 1 (0.0172 mol), and the reaction was stirred for three hours at room temperature. The solution was cooled in an ice bath, placed under an atmosphere of N2, and diphenylphosphine chloride 2 (2.87 mL, 3.44 g, 0.016 mmol) was added dropwise. The reaction was stirred overnight at room temperature. The reaction solution was decanted away from the magnesium turnings into a separatory funnel, and the round bottom flask was rinsed with ether. Water was added to the separatory funnel, and after shaking the solution the pH of the aqueous layer was neutralized with either 3 M NaOH or 3 M HCl. In the case of emulsion formation, saturated NaCl can be added to aid in the separation of the layers. The organic layer was separated, washed three times with water, dried over anhydrous sodium sulfate and concentrated under reduced pressure to give the product as a colored oil or low-melting solid, typically light amber, and occasionally light green (80% average yield). If an oil is obtained, it will often crystallize upon standing overnight. ¹H NMR (300 MHz, CDCl₃): δ 7.60 (m, 1H), 7.48–7.26 (m, 11H), 7.15 (m, 1H); ¹³C NMR (75 MHz, CDCl₃): δ 138.2 (d, J_{C-P} = 27 Hz), 138.1 (d, J_{C-P} = 9 Hz), 136.5 $(d, J_{C-P} = 26 \text{ Hz}), 133.2 (d, J_{C-P} = 20 \text{ Hz}), 132.2, 129.0, 128.6 (d, J_{C-P} = 20 \text{ Hz})$ $J_{C-P} = 8 \text{ Hz}$), 128.2 (d, $J_{C-P} = 8 \text{ Hz}$); ³¹P NMR (161 MHz, CDCl₃): δ –18.9; FT-IR (cm⁻¹): ν 1403, 972, 683.

Diphenyl(2-thienyl)phosphine oxide 4. Phosphine 3 (4.12 g, 1.18 mmol) was added to a round bottom flask and dissolved in 12 mL of DMSO (0.168 mol). The molybdenum catalyst MoO₂Cl₂(DMSO)₂ was added as a solid (0.208 g, 0.59 mmol), and the reaction was stirred at 100 °C for twenty minutes. The solution was allowed to cool to room temperature, and was poured into 60 mL of 1 M NaOH. The resultant white, cloudy solution was filtered via a Büchner funnel to give the crude product as a mixture of white and pink solids. This crude product (3.33 g) was purified by dissolution in hot methanol (ca. 13 mL) and precipitation with water (ca. 10 mL) to give the target phosphine oxide as a white solid (65% yield). Occasionally activated charcoal was added during this recrystallization step to remove colored impurities. Crystals suitable for analysis by X-ray diffraction were formed by slow evaporation of the product from CDCl₃. The characterization details below agree with previous reports.31 1H NMR (400 MHz, CDCl₃): δ 7.75–7.70 (m, 4H), 7.58–7.26 (m, 7H), 7.21–7.18 (m, 2H); 1 H NMR (400 MHz, CD₃CN): δ 7.87 (m, 1H), 7.72–7.46 (m, 10H), 7.38 (m, 1H), 7.22 (m, 1H); 13 C NMR (75 MHz, CDCl₃): δ 137.0 (d, J_{C-P} = 10 Hz), 133.9 (d, J_{C-P} = 111 Hz), 134.0 (d, J_{C-P} = 5 Hz), 133.7 (s), 132.3 (d, J_{C-P} = 3 Hz), 131.8 (d, J_{C-P} = 10 Hz), 128.6 (d, J_{C-P} = 13 Hz), 128.3 (d, J_{C-P} = 14 Hz); ³¹P NMR (161 MHz, CDCl₃): δ 23; ³¹P NMR (161 MHz, CD₃CN): δ 19.8; mp: 116–117 °C; FT-IR (cm⁻¹): ν 1402, 1177 (P=O).

Diphenyl(2-thienyl)phosphine sulfide 5. Phosphine 3 (500 mg, 2.42 mmol) and solid sulfur (80 mg, 2.42 mmol) were mixed in 10 mL chloroform for 60 minutes. A second batch of

sulfur was added (56 mg, 1.75 mmol) and the mixture was stirred for another hour. The reaction mixture was then filtered through a pad of Celite and concentrated under reduced pressure to give the crude product as a solid (578 mg). The product was suspended in hot isopropanol (75 °C, ca. 10 mL) to which DMSO was added dropwise until complete dissolution occurred (ca. 5 mL). The solution was allowed to cool to room temperature, at which point the product crystallized as white snowflakes (423 mg, 73% recovered yield). Crystals suitable for analysis by X-ray diffraction were formed by slow evaporation of the product from CDCl₃. ¹H NMR (400 MHz, CDCl₃): δ 7.88–7.71 (m, 4H), 7.54–7.42 (m, 7H), 7.16 (m, 2H); ¹³C NMR (75 MHz, CDCl₃): 137.2 (d, J_{C-P} = 10 Hz), 135.5 (d, $J_{C-P} = 93 \text{ Hz}$), 134.5 (d, $J_{C-P} = 5 \text{ Hz}$), 133.7 (d, $J_{C-P} = 89 \text{ Hz}$), 131.9 (d, J_{C-P} = 4 Hz), 131.8 (s), 128.6 (d, J_{C-P} = 13 Hz), 128.4 (s); 31 P NMR (161 MHz, CDCl₃): δ 35; mp: 113–126 °C.

Diphenyl(2-thienyl)phosphine selenide 6. Phosphine 3 (500 mg, 2.42 mmol) and solid selenium (190 mg, 1.86 mmol) were stirred in 10 mL chloroform for 60 minutes. The reaction mixture was filtered through a bed of Celite, then concentrated under reduced pressure to give a white solid. The crude product stirred in boiling isopropanol (ca. 10 mL), to which DMSO was added dropwise until all of the solid had dissolved (ca. 5-10 mL). The solution was allowed to cool to room temperature, and the product precipitated as a white, flaky solid which was isolated by vacuum filtration (380 mg, 65% recovered yield). A second crop of the product may be obtained from the mother liquor, with a relatively low yield (40 mg, 7% additional yield). Crystals suitable for analysis by X-ray diffraction were formed from slow evaporation of the product from CDCl₃. ¹H NMR (400 MHz, CD₃CN): δ 7.95–7.26 (m, 13H); ³¹P NMR (161 MHz, CDCl₃): δ 23 (Se satellites J_{Se-P} = 734 Hz); ⁷⁷Se³² NMR (76 MHz, CDCl₃): δ –232.6 (d, ${}^{1}J_{P-Se}$ = 739 Hz); mp: 149.3-150.7 °C.

Complexes of phosphine oxide 4 with lanthanide nitrate hydrates. General procedure. A round bottom flask was charged with the phosphine oxide 4 (3 molar equivalents, generally between 25–50 mg) and *ca.* 15 mL acetonitrile. The Ln (NO₃)₃ hydrate (1 molar equivalent) was added to the reaction as a solid, and the solution was stirred at room temperature for 30 minutes. The volatiles were removed under reduced pressure to give the complexes as colorless solid powders or solid films on the surface of the round bottom flask. The complexes were triturated 2–3 times with diethyl ether (5–10 mL) and placed under high vacuum over night to remove any residual solvents. Typical isolated yields of the complexes were 85–90% as powders.

[La(4)₃(NO₃)₃] complex. ¹H NMR (400 MHz, CD₃CN): δ 7.68–7.60 (m, 5H), 7.54–7.47 (m, 3H), 7.38–7.31 (m, 4H), 7.08–7.04 (m, 1H); ³¹P NMR (161 MHz, CD₃CN): 27; FT-IR (cm⁻¹): ν 1150 (P=O); ESI-LRMS (M⁺, m/z): calcd for [La (C₁₆H₁₃OPS)₂(NO₃)₂(CH₃CN)]⁺ 872.0, found 872.1; CHN analysis calculated (found) for La(C₁₆H₁₃OPS)₃(NO₃)₃(H₂O): C 48.21 (48.08), H 3.46 (3.31), N 3.51 (3.74).

[$Pr(4)_3(NO_3)_3$] complex. FT-IR (cm⁻¹): ν 1149 (P=O); ESI-LRMS (M⁺, m/z): calcd for [$Pr(C_{16}H_{13}OPS)_3(NO_3)_1(CH_3CN)_2$]²⁺ 568.5,

found 568.6; CHN analysis calculated (found) for Pr $(C_{16}H_{13}OPS)_3(NO_3)_3(H_2O)_{2.5}$: C 47.07 (46.80), H 3.62 (3.38), N 3.43 (3.97).

[$Sm(4)_3(NO_3)_3$] complex. FT-IR (cm⁻¹): ν 1149 (P=O); ESI-LRMS (M⁺, m/z): calcd for [$Sm(C_{16}H_{13}OPS)_2(NO_3)_2(CH_3CN)$]⁺ 882.0, 885.0, 887.0, found 881.9, 884.9, 886.9; CHN analysis calculated (found) for $Sm(C_{16}H_{13}OPS)_3(NO_3)_3(H_2O)_5$: C 43.83 (43.51), H 4.06 (3.96), N 3.19 (3.29).

[$Tb(4)_3(NO_3)_3$] complex. ¹H NMR (400 MHz, CD₃CN): extremely broad; FT-IR (cm⁻¹): ν 1156 (P=O); ESI-LRMS (M⁺, m/z): calcd for [$Tb(C_{16}H_{13}OPS)_2(NO_3)_2(CH_3CN)$]⁺ 892.0, found 892.1; CHN analysis calculated for $Tb(C_{16}H_{13}OPS)_3(NO_3)_3(H_2O)_5(CH_3CN)$: C 45.20 (44.76), H 3.94 (3.32), N 4.22 (4.19).

[Lu(4)₃(NO₃)₃] complex. ¹H NMR (400 MHz, CD₃CN): δ 7.77–7.61 (broad), 7.60–7.35 (broad), 7.18 (broad); ³¹P NMR (161 MHz, CD₃CN): δ 31; FT-IR (cm⁻¹): ν 1153 (P=O); ESI-LRMS (M⁺, m/z): calcd for [Lu(C₁₆H₁₃OPS)₂(NO₃)₁(CH₃CN)]²⁺ 423.3, found 422.0; CHN analysis calculated (found) for Lu (C₁₆H₁₃OPS)₃(NO₃)₃(H₂O)₃(CH₃CN): C 45.88 (45.80), H 3.70 (3.26), N 4.28 (3.99).

Complexes of phosphine oxide 4 with lanthanide triflates. General procedure. Phosphine oxide 4 (three molar equivalents, around 50 mg) and the $Ln(OTf)_3$ (one molar equivalent) were ground together in the solid state using a mortar and pestle. The mixed solid was transferred to a round bottom flask, and heated using a wax bath until the mixture melted (typically around 135 °C) and resolidified (typically around 155 °C). The solid complexes were used without further purification.

[La(4)₃(OTf)₃] complex. ¹H NMR (400 MHz, CDCl₃): δ 7.70–7.50 (m, 8H), 7.40–7.30 (m, 4H), 7.07–7.05 (m, 1H); ³¹P NMR (161 MHz, CDCl₃): 29; FT-IR (cm⁻¹): ν 1151 (P=O); ESI-LRMS (M⁺, m/z): calcd for [La(C₁₆H₁₃OPS)₂(OSO₂CF₃)₁(CH₃CN)]²⁺ 448.5, found 448.1; CHN analysis calculated (found) for La (C₁₆H₁₃OPS)₃(OSO₂CF₃)₃(H₂O)₇: C 39.14 (38.44), H 3.41 (2.73), N 0.00 (0.00).

[Sm(4)₃(OTf)₃] complex. 1 H NMR (400 MHz, CDCl₃): δ 7.95–7.80 (m, 6H), 7.58 (m, 2H), 7.38 (m, 4H), 7.09 (m, 1H); 31 P NMR (161 MHz, CDCl₃): 28; FT-IR (cm $^{-1}$): ν 1131 (P=O); ESI-LRMS (M $^{+}$, m/z): calcd for [Sm(C₁₆H₁₃OPS)₂(OSO₂CF₃)₁] $^{2+}$ 433.0, 434.5, 435.5 found 433.1, 434.1, 435.3; CHN analysis calculated (found) for Sm(C₁₆H₁₃OPS)₃(OSO₂CF₃)₃(H₂O)₄: C 40.23 (40.27), H 3.11 (3.17), N 0.00 (0.22).

 $[Tb(4)_3(OTf)_3]$ complex. FT-IR (cm⁻¹): ν 1132 (P=O); ESI-LRMS (M⁺, m/z): calcd for $[Tb(C_{16}H_{13}OPS)_1(OSO_2CF_3)_1(CH_3CN)(H_2O)_2]^{2+}$ 334.5 found 334.5; CHN analysis calculated (found) for Tb $(C_{16}H_{13}OPS)_3(OSO_2CF_3)_3$: C 41.99 (41.88), H 2.69 (2.91), N 0.00 (0.00).

[$Yb(4)_3(OTf)_3$] complex. FT-IR (cm⁻¹): ν 1135 (P=O); ESI-LRMS (M⁺, m/z): calcd for [$Yb(C_{16}H_{13}OPS)_1(OSO_2CF_3)_1(CH_3CN)_1(H_2O)_3$]²⁺ 350.5, found 349.9; CHN analysis calculated (found) for Yb (C₁₆H₁₃OPS)₃(OSO₂CF₃)₃(H₂O)₉: C 37.46 (37.26), H 3.51 (3.30), N 0.00 (0.00).

Results and discussion

Synthesis of ligands and metal-ligand complexes

Synthesis of diphenyl(2-thienyl)phosshine 3 and the chalcogenide derivatives 4–6. Triarylphosphines are advantageous in organo-phosphine coordination chemistry in that they are relatively stable to ambient air oxidation to the phosphine oxides, much unlike the alkylphosphines. We have chosen to incorporate the 2-thienyl group as one of the aromatic rings on the phosphorus atom due to its stability and resistance to oxidation. Furthermore, the location of the sulfur atom in this heteroaromatic ring may allow for it to interact with a Ln or An metal that is bound through the ligands P—O group.

The synthesis of the target compound diphenyl(2-thienyl) phosphine (3, Scheme 1) appears in a variety of publications. Many prior syntheses cite the use of lithiated thiophene as the nucleophile in the reaction with chlorodiphenylphosphine. 33-38 Horner and Roder employed Grignard chemistry, with a high level of success, that used iodothiophene as the starting material. Diphenyl(2-thienyl)phosphine 3 has also been made as an example of reaction scope in the demonstration of other general, catalytic methods. In all of these previously published methods, the Grignard chemistry appears to be the most user-friendly and has given the highest isolated yields of product. In this work we have chosen to use chemistry similar to Horner and Roder, and our preparation is novel only in that we use 2-bromothiophene as the starting material.

The synthesis begins with the generation of the Grignard reagent from commercially available 2-bromothiophene 1 and magnesium. From here, chlorodiphenylphosphine 2 is added

Scheme 1 Synthesis of phosphine 3 and chalcogenide derivatives 4-6.

slowly to the Grignard reagent. This slow addition is necessary to obtain the phosphine in good yield. It is not necessary to remove unreacted magnesium metal from the reaction mixture, and these conditions consistently generate the desired diphenyl(2-thienyl)phosphine 3 in >70% recovered yield as an oil or low-melting solid.

Use of the thienyl-group as a supporting ligand for phosphine complexes is advantageous in that the thienyl group is known to be highly resistant to oxidation. As is elaborated in a few, detailed studies, ^{45–47} the sulfur of thiophene will remain stubbornly inert under chemical conditions where one would normally expect other organo-sulfur functional groups to oxidize to sulfoxides or sulfones. Thus, we can confidently use a variety of approaches to selectively oxidize the phosphorus atom of phosphine 3, without altering the thienyl group.

The phosphine oxide 4 has been independently synthesized using a number of varied reaction conditions that involve the coupling of a thiophene-derivative with diphenylphosphine oxide in the presence of a metal catalyst. ^{31,48–53} Other groups have exploited decarbonylation reactions in the presence of $Pd(0)^{54}$ or $Pd(0)^{54}$

In this work, the oxide 4 was prepared using the $\mathrm{Mo^{6^+}}$ catalyst $\mathrm{MoO_2Cl_2(DMSO)_2}$ (DMSO = dimethylsulfoxide) as described by Arnáiz and Aguado. Methods for the chalcogenation of phosphines (P = X, X = S, Se, Te) are varied, and many examples date rather early in the literature. Our method is most similar to that of Grim and Walton, and perhaps only more efficient in our hands due to the higher purity of S and Se powders now available. The sulfide 5 and selenide 6 were prepared by stirring the free phosphine in chloroform with one equivalent of elemental sulfur or selenium, respectively.

The phosphine 3 and chalcogenide derivatives 4–6 were characterized by NMR (1 H, 13 C, 31 P), LR-MS and IR. The 1 H NMR spectra of all four compounds 3–6 contain multiplets in the aromatic region that are only interpretable for the thienyl group. The 31 P NMR spectra, however, are comprised of one singlet resonating at the expected chemical shifts: phosphine 3: -18.9 ppm; oxide 4: +23 ppm; sulfide 5: +35 ppm; selenide 6: +23 ppm, with 77 Se satellites ($I_{Se-P} = 734$ Hz).

The oxide, sulfide and selenide derivatives 4, 5 and 6 were also characterized by single crystal X-Ray diffraction (Fig. 2). The P=O, P=S and P=Se bond lengths were 1.514(3), 1.9573 (11) and 2.1132(12) Å, respectively. The geometry around the phosphorus atom of all three structures is close to an ideal tetrahedron, with τ_4 descriptors for four-fold coordination of 0.96 (oxide), 0.95 (sulfide) and 0.96 (selenide; where 1.00 = perfect tetrahedron and 0.00 = perfect square planar). 61 For all three structures the largest bond angles around the phosphorus atom are those that involve the chalcogenide atom (X), with C-P-X bond angles around 113°. Crystal data and structure refinement information is given in Table 1 for the structures of 4, 5 and 6, as well as selected bond lengths and angles in Table 2. Additional data tables for these structures and descriptions of the treatment of any disordered electron density are given in the ESI.†

Synthesis and characterization of complexes between phosphine oxide 4 and $Ln(NO_3)_3$. The lanthanide nitrate complexes with phosphine oxide 4 were formed by stirring three equivalents of the ligand with one equivalent of the $Ln(NO_3)_3$ hydrate at room temperature in acetonitrile. This metal-ligand stoichiometry was chosen due to precedents by previous groups. The complexes were isolated as a thin oil after removal of the solvent, which were triturated with a small amount of diethyl ether to give a powder. The complexes are stable for months when stored on the shelf.

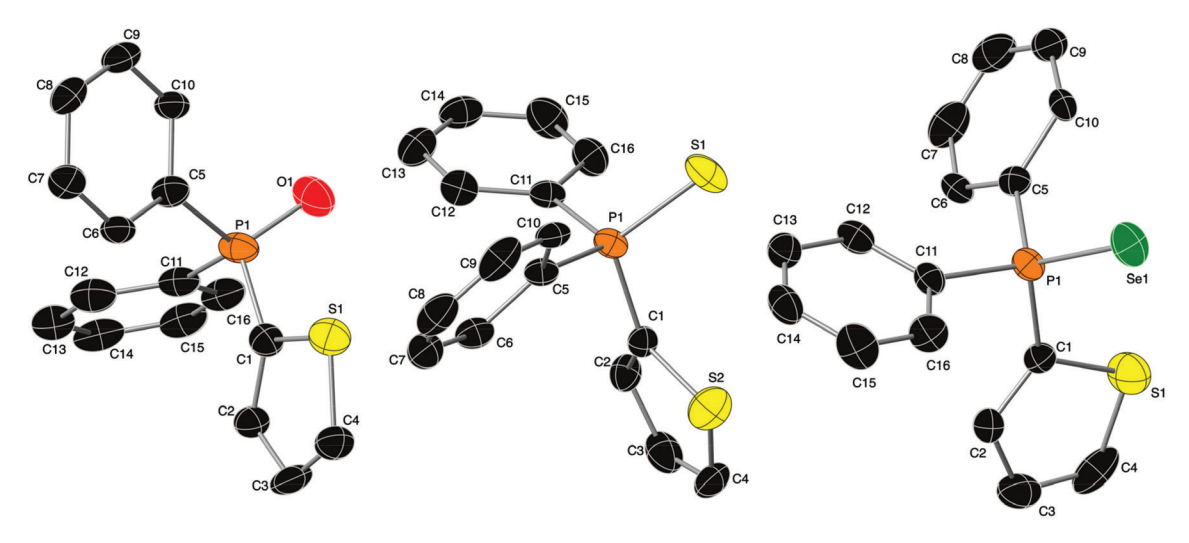


Fig. 2 X-Ray crystal structures of compounds 4, 5 and 6 (from left to right) using standard CPK colors, along with the atom numbering scheme. Thermal ellipsoids are shown at the 50% probability level, and all hydrogen atoms have been omitted for clarity. For compound 4, only the major component is shown.

Analysis of the 1:3 [Ln(4)₃(NO₃)₃] complexes by low resolution ESI-MS was carried out by introduction of the complexes as a dilute solution in acetonitrile. The MS spectra show peaks corresponding to complexes with one, two or three ligands per Ln metal, and often times as an adduct with water or CH₃CN. Ionization occurred through loss of either one or two nitrate anions to give mono- and dicationic species.

To explore the solution behavior of the $[Ln(4)_3(NO_3)_3]$ complexes, ¹H and ³¹P NMR were collected under a number of conditions. In the ¹H NMR spectrum (CD₃CN) of the free phosphine oxide ligand 4, the phenyl-ring signals comprise a complicated multiplet spanning ~0.7 ppm centered at 7.5 ppm, with distinct 2-thienyl multiplets at 7.87, 7.38 and 7.22 ppm. The chemical shift of this multiplet is largely unchanged and slightly broadened in the ¹H NMR spectra of the La³⁺ and Lu³⁺ complexes (Fig. 3). The signals in the ¹H NMR spectra of the other complexes that were studied (Ln = Pr³⁺, Sm³⁺, Tb³⁺) were severely broadened. Analysis of the La³⁺ and Lu³⁺ complexes by ³¹P NMR shows one signal that is shifted downfield slightly from that of the free ligand ($\Delta \delta = 4$ and 8 ppm, respectively). This downfield shift represents a decrease in electron density around the phosphorus atom upon Ln3+ complexation, which is consistent with the donation of electron density from the P=O group to form the O…Ln dative bond.

To gain insight into the speciation of the complexes in solution, we carried out a titration of the free ligand with incremental amounts of La(NO₃)₃·(H₂O)₆ in CD₃CN and analyzed these solutions with ¹H and ³¹P NMR (Fig. 3). The signals in the ¹H NMR spectrum (400 MHz, CD₃CN) were assigned with the assistance of the prediction tool in MestReNova. ⁶² The individual spectra progress from excess ligand (six equivalents) to excess metal (1.5 equivalents). For all spectra only one set of resonances are observed, which indicates that the metal and ligand are undergoing exchange that is fast on the ¹H NMR time scale.

Analysis of the same solutions by 31P NMR (161 MHz, CD₃CN) reveals slightly different behavior. Here, the singlet that corresponds to the phosphorus atom of the ligand broadens upon addition of La(NO₃)₃·(H₂O)₆ in solutions where there is a significant excess of ligand (five or six equivalents). We interpret this broadening to be from the presence of a significant amount of free ligand in solution, and a rate of ligand exchange that is intermediate on the ³¹P NMR time scale. The ³¹P NMR spectrum of the solution with a 1:3 La³⁺-ligand ratio shows a sharper signal that is shifted downfield from free ligand ($\Delta \delta$ 8 ppm), and represents the average resonance from a solution where most of the ligands are complexed to a metal. The chemical shift of the 31P NMR signal stabilizes upon addition of another equivalent of metal (1:2 La³⁺-ligand ratio) to give a sharp singlet that does not shift downfield when more metal is added. We interpret these results as an indication that the speciation of the complexes is fluxional in solu-

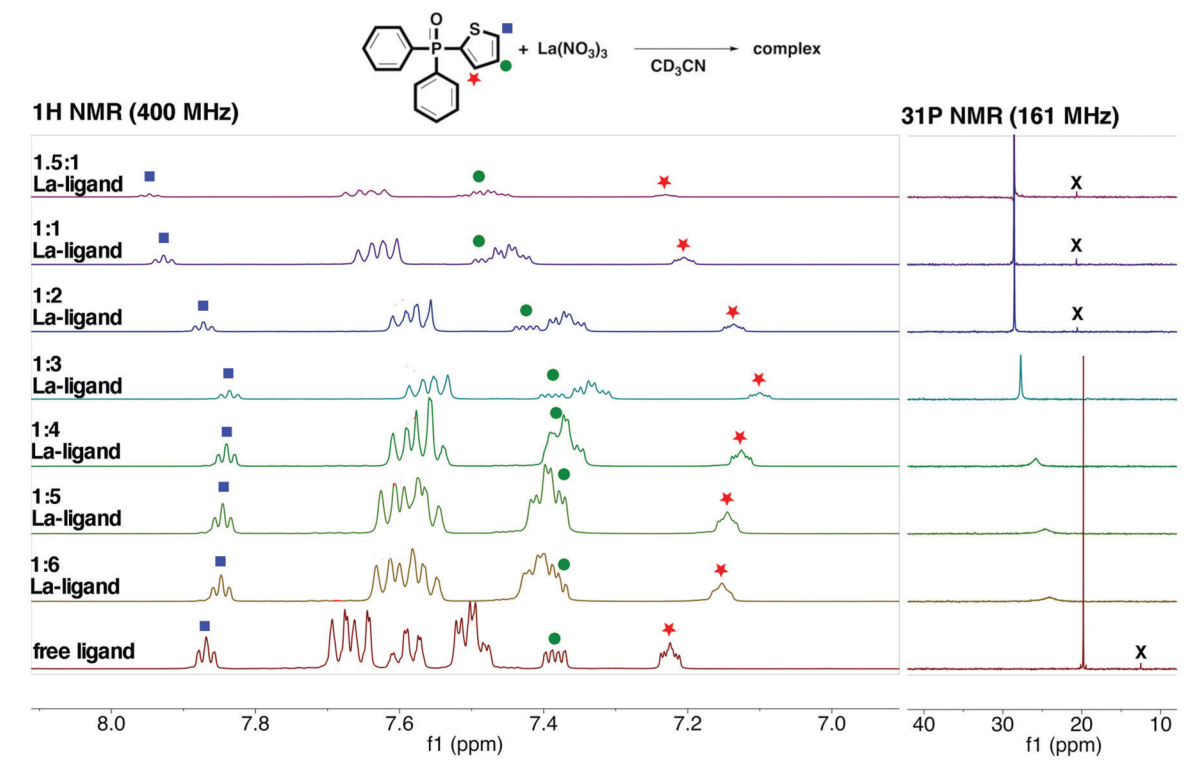


Fig. 3 NMR spectra of the titration of ligand 4 (10 mg in 0.75 mL CD₃CN) with La(NO₃) $_3$ ·(H₂O)₆ (1.0 M in CD₃CN) to give varying stoichiometries of metal to ligand in solution. In the 1 H NMR spectrum the resonances corresponding to the hydrogen atoms of the thienyl ring are labeled according to the diagram shown; resonances corresponding to the hydrogen atoms of the phenyl rings are unlabeled. The signal marked with a 'x' in the 31 P NMR spectrum corresponds to a minor impurity.

tions of acetonitrile, and that it is likely that no more than three or four ligands coordinate directly to the metal when nitrate is the counteranion. This coincides with the analysis of 1:3 Ln-ligand 4 complexes *via* X-Ray diffraction (*vide infra*).

In the solid state, the complexes were characterized by IR and X-Ray crystallography. The IR spectrum of the free phosphine oxide 4 shows a P=O stretch at 1185 cm⁻¹. The frequency of the P=O stretch in the IR spectra of the [Ln $(4)_3(NO_3)_3$] complexes moves to lower wavenumbers ranging from 1149–1156 cm⁻¹ ($\Delta\nu$ = 36–29 cm⁻¹). This shift represents a weakening of the P=O bond, which is again consistent with the donation of electron density from this bond to form the O···Ln bond.

Single crystals of the $Ln(4)_3(NO_3)_3$ complexes were grown by vapor diffusion of either diethyl ether or benzene into a solution of the complex in acetonitrile. Analysis of these crystals by X-ray diffraction revealed a 1:3 ratio between the metal and the ligand with three bidentate nitrate anions completing the inner coordination sphere.

For the complexes where Ln = La, Pr and Sm the X-ray diffraction structures are isomorphic and were solved in the high symmetry space group $R\bar{3}$ (Fig. 4). The electron density corresponding to every atom in the structures, other than the metal center, was disordered. A detailed description of how this complete molecular disorder was treated can be found in the ESI.† The geometry of these nine-coordinate structures resembles a tricapped trigonal prism as defined by Alvarez and coworkers. Analysis of the inner-coordination sphere using the program SHAPE⁶⁴ is consistent with this description.

The model of the La³⁺ complex is shown in Fig. 4 as a representative example, along with the atom labelling scheme. In

each complex the electron density corresponding to the thienyl ring was disordered. This disorder was modeled as two rotational isomers around the P1-C1 bond, with occupancy ratios of 84:16 for the La³⁺ complex, and 70:30 for the Sm³⁺ complex. This disorder was relatively minor in the Pr3+ complex and was not modeled, in part, due to a poor data-toparameter ratio. Due to the high symmetry of the diffraction data, it is not possible to determine the combination of individual thienyl ring orientations in each complex, so we have modeled only the extremes. The orientation of the three thienyl rings where the sulfur atom points toward the other ligands as shown in Fig. 4, is one extreme and can be described as "sulfur-in". This orientation represents the major component of the disordered electron density. The other extreme is where the sulfur atom of each thienyl ring points away from the other ligands and can be described as "sulfurout" (not shown). For the "sulfur-in" orientation of the thienyl rings, an intramolecular sulfur- $\pi^{65,66}$ interaction is observed between the aromatic rings. In the "sulfur-out" orientation, a CH- π interaction is present between the thienyl rings of the ligands. The calculated S-centroid and CH-centroid distances are ~3.3 and ~2.5 Å, respectively. Crystal data and structure refinement information is given in Table 3 for all [Ln (4)₃(NO₃)₃] structures reported here, as well as selected bond lengths and angles in Table 4. Figures depicting the thermal ellipsoids and atom labeling scheme for all [Ln(4)3(NO3)3] structures are given in the ESI.†

Analysis of the bond lengths and angles for this series of complexes reveals typical trends as seen for Ln complexes (Table 4). We note here that the R1 values for each structure are greater than 5%, but less than 10%, hence there are limits

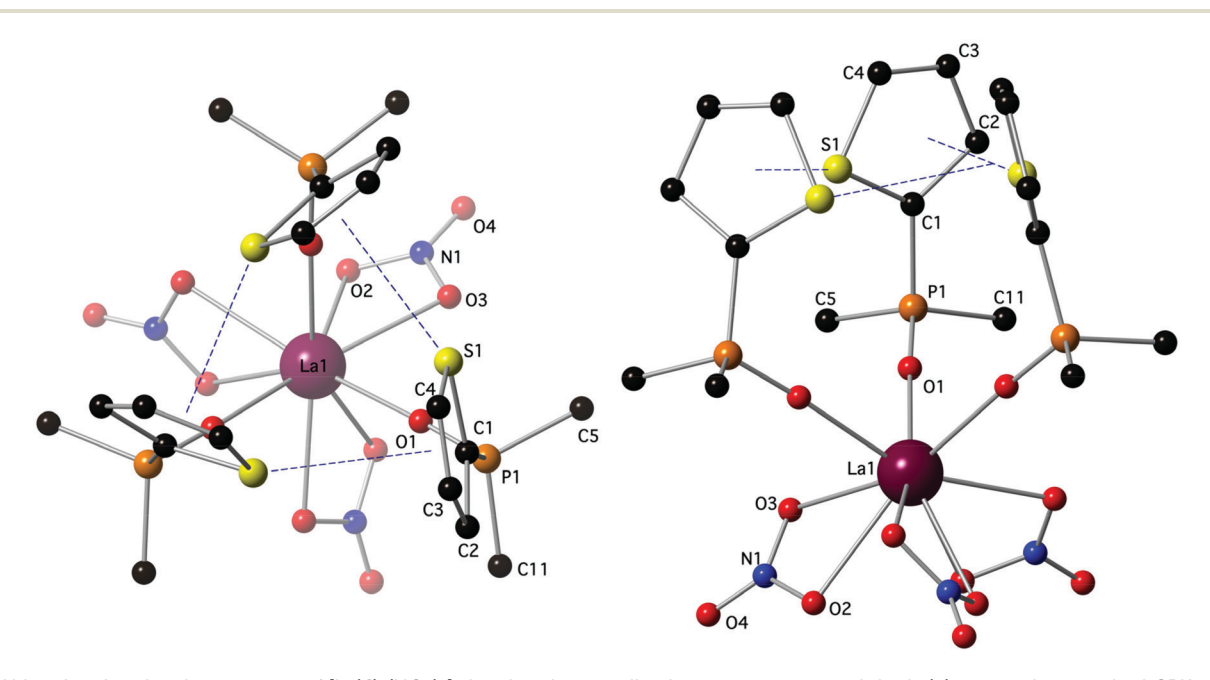


Fig. 4 Abbreviated molecular structure of $[La(4)_3(NO_3)_3]$ showing the coordination geometry around the La(III) atom using standard CPK colors (La = dark purple). Sulfur- π interactions are depicted with a blue, dashed line. For clarity, only the major component of the disordered thienyl ring is shown, all hydrogen atoms and the pendant phenyl rings have been omitted. The complete molecular structures of the La³⁺, Pr³⁺ and Sm³⁺ complexes showing thermal ellipsoids are provided in the ESI.†

 Table 3
 Crystal data and structure refinement information for the crystal structures described in this paper

Structure	$\mathrm{La}(4)_3(\mathrm{NO}_3)_3$	$\Pr(4)_3(\mathrm{NO}_3)_3$	$\mathrm{Sm}(4)_3(\mathrm{NO}_3)_3$	$Tb(4)_3(NO_3)_3 (C_6H_6)$	${\rm Er}(4)_3({ m NO}_3)_3({ m C}_6{ m H}_6)$	$\mathrm{Tb}(4)_4(\mathrm{OTf})_3$
CCDC number Empirical formula Formula weight Temperature/K Crystal system Space group a/Å b/Å c/Å a/A a/O Volume/ų Z Z Reflections Reflections	1846830 C ₄₈ H ₃₉ LaN ₃ O ₁₂ P ₃ S ₃ 1177.80 173(2) Trigonal R ³ 19.720(5) 11.549(3) 90 120 3890(2) 3 9924	1922657 C ₄₈ H ₃₉ N ₃ O ₁₂ P ₃ PrS ₃ 1179.80 173(2) Trigonal R ³ 19.836(11) 11.610(6) 90 90 120 3956(5) 3	1922734 C ₄₈ H ₃₉ N ₃ O ₁₂ P ₃ S ₃ Sm 1189.24 173(2) Trigonal R ³ 19.608 11.469(5) 90 120 3819(4) 3 10.213	2173564 C ₅₄ H ₄₅ N ₃ O ₁₂ P ₃ S ₃ Tb 1275.94 100.00(10) Orthorhombic Pbca 20.75550(10) 17.56580(10) 30.25370(10) 90 90 90 11.030.10(9) 88	2173657 C ₅₄ H ₄₅ ErN ₃ O ₁₂ P ₃ S ₃ 1284.28 100.00(10) Orthorhombic Pbca 20.75560(10) 17.56230(10) 30.2522(2) 90 90 11 1027.41(11)	1850479 C _G ,H ₃₂ F ₉ O ₁₃ P ₄ S ₇ Tb 1743.30 173(2) Triclinic Pi 13.7126(11) 14.5867(12) 19.8641(17) 86.1680(10) 71.5830(10) 89.4960(10) 3761.0(5) 2
Independent reflections Final R indexes [I	1595 $[R_{\text{int}} = 0.0607, R_{\text{sigma}}]$ = 0.0381 $R_1 = 0.0906, WR_2 = 0.2957$	1778 $[R_{\text{int}} = 0.0790, R_{\text{sigma}}]$ = 0.0660] $R_1 = 0.0947, wR_2 = 0.2897$	1577 $[R_{\text{int}} = 0.0912, R_{\text{sigma}}]$ = 0.0598 $]$ $R_1 = 0.0769, wR_2 = 0.2368$	11 654 $[R_{\rm int} = 0.0353, R_{\rm sigma}]$ = 0.0226] $R_1 = 0.0608, wR_2 = 0.1612$	11 680 $[R_{\text{int}} = 0.0386, R_{\text{sigma}} 0.024=]$ $R_1 = 0.0686, wR_2 = 0.1712$	13 819 $[R_{\rm int}=0.0467,R_{\rm sigma}=0.0410]$ $R_1=0.0537,WR_2=0.1459$
Final R indexes [all data] Solvent masks	$R_1 = 0.0910$, w $R_2 = 0.2962$	$R_1 = 0.0964$, $wR_2 = 0.2915$	$R_1 = 0.0782$, w $R_2 = 0.2379$	$R_1 = 0.0636$, w $R_2 = 0.1640$	$R_1 = 0.0722$, w $R_2 = 0.1738$	$R_1 = 0.0636, \text{ w} R_2 = 0.1563$
						44.5 electron count

to the amount of information that should be inferred from comparison of bond length and angle data. The Ln-O1(P1) bond length between the phosphine oxide oxygen atom (O1) and the metal center decreases from 2.455(18) to 2.388(19) Å as the size of the metal decreases. The Ln-O bond lengths for the nitrate group, however, remain relatively consistent across the series and range from 1.26(3)-1.29(3) Å. The O-Ln-O bond angle between two phosphine oxide ligands ranges from 87.0 $(6)-88.2(7)^{\circ}$.

In order to align discussion of the structures reported here with previous work by other research groups, 16,67 we can consider each of the bidentate nitrate groups as a stereochemically mono-coordinated ligand that associates to the metal through its' center of gravity (the nitrogen atom, Fig. 5). This will allow us to describe the stereochemistry of these complexes as facial isomers of a six-coordinate octahedron. This facial stereochemistry has previously been observed in one complex of Ln (III) nitrate with triphenylphosphine oxide⁶⁷ as well as in complexes with the less sterically demanding diphenylmethylphosphine oxide. 32 Ln(NO₃)₃-ligand complexes reported in the literature where the ligand has bulkier groups bonded to the phosphorus atom (e.g. cyclohexyl,⁶⁸ iso-butyl,⁶⁹ iso-propyl⁷⁰ consistently have crystal structures with a meridional arrangement of the phosphine oxide ligands around the metal center. Lastly, Levason and co-workers have reported complexes of La³⁺ and Lu³⁺ with triphenylphosphine oxide with a 1:4 Lnligand ratio by including six equivalents of the ligand in the reaction mixture.71

For the $[Ln(4)_3(NO_3)_3]$ complexes where Ln = Tb and Er the X-ray diffraction structures are isomorphic with one another but different than those described above. These data were solved in the orthorhombic space group *Pbca*, and the asymmetric unit contained one molecule of solvent benzene. The electron density corresponding to the carbon and sulfur atoms of the ligand was highly disordered, and was modeled over two parts as both rotational and positional isomers of the thienyl ring. The disordered electron density was so severe that the carbon atoms were left as isotropic in the final model (Fig. 6). The atoms of the inner-coordination sphere (metal, P=O atoms of the ligand, and all atoms of the nitrate groups) were ordered in the structure. Crystal data and structure refinement information is given in Table 3 for these [Ln(4)3(NO3)3] structures, as well as selected bond lengths and angles in Table 4. Figures depicting the thermal ellipsoids and atom labeling schemes are given in the ESI.†

A closer look at the inner coordination sphere reveals a strictly nine-coordinate metal, the same as observed in our previous [Ln(Ar₃P=O)₃(NO₃)₃] complexes described above (bidentate nitrates) (Fig. 6, center). If the bidentate nitrate groups are still to be considered stereochemically mono-coordinated ligands (Fig. 6, right) the structure can be described as a distorted octahedron. Interestingly, the six ligands for these structures (Ln = Tb, Er) are arranged in a meridional stereochemistry around the metal center, as opposed to the facial stereochemistry observed for the complexes where Ln = La, Pr and Sm. One possible reason for the different geometry observed

Table 4 Selected bond lengths (Å) and angles (°) for the [Ln(4)₃(NO₃)₃] crystal structures

Ln	La	Pr	Sm	Tb	Er
Ln-O(P)	2.455(18)	2.418(18)	2.388(19)	2.280^{a}	2.280^{a}
Ln-O(nitrate)	2.66(2)	2.597(19)	2.493(17)	2.480^{a}	2.480^{a}
	2.614(18)	2.61(2)	2.553(17)		
P-O	1.482(19)	1.517(18)	1.472(19)	1.480^{a}	1.497^{a}
N-O(Ln)	1.29(3)	1.29(2)	1.29(3)	1.264^{a}	1.258^{a}
	1.29(3)	1.26(3)	1.27(3)		
S1-Cg1 ⁱ	3.340(13)	3.351(13)	3.32(2)	_	_
$O(P)$ -Ln- $O(P)^{i}$	87.9(6)	88.2(7)	87.0(6)	152.98(11)	153.01(13)
				82.67(12)	83.06(14)
				82.90(12)	82.64(13)
N-Ln-N ⁱ	94.1(6)	93.6(6)	94.2(6)	96.20(12)	96.16(13)
				171.26(12)	171.27(14)
				78.33(11)	78.38(13)

For structures where Ln = La, Pr, Sm: symmetry code: i: 1 + y - x, 1 - x, + z. These numbers are average bond lengths and angles.

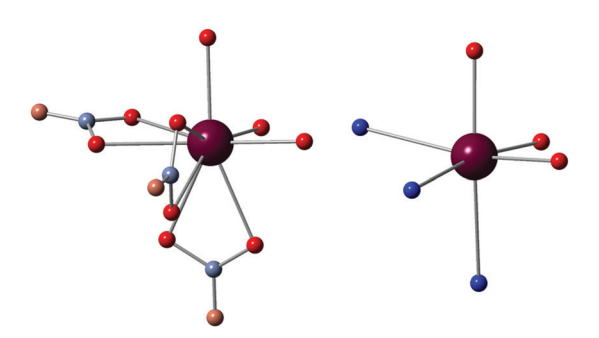


Fig. 5 The metal coordination sphere of the $[Ln(4)_3(NO_3)_3]$ crystal structures (Ln = La, Pr, Sm). Left: all nine oxygen atoms (red) that coordinate to the metal (nitrogen and non-coordinating oxygen atom of the nitrate groups are depicted with lighter blue and red colors); Right: depiction of the bidentate nitrates as monodentate ligands through the nitrogen atom to give a six-coordinate metal (octahedral geometry).

here is that La, Pr and Sm have larger ionic radii than Tb and Er. The larger ionic radii may allow the phenyl and thienyl rings of the ligands to adopt a different orientation upon binding to the metal, which when combined with the intramolecular S-pi and CH-pi interactions of the complex made this geometry more favorable in the solid state. Alternatively, a *meridional* arrangement of ligands allows them to be more spread out around the metal center, and it is possible that this arrangement was necessary with the smaller Tb and Er metals. The isolation of Ln-ligand complexes of (4) with variable stoichiometry and stereochemical arrangements of coordinating groups is supported by our observations of the fluxional nature of these metal-ligand complexes in solutions of acetonitrile.

Synthesis and characterization of complexes between phosphine oxide 4 and Ln(OTf)₃. The lanthanide triflate complexes were formed by a melt reaction between three equivalents of the phosphine oxide 4 and the corresponding Ln(OTf)₃. A ratio of three ligands to each metal was chosen due to our previous work with the lanthanide nitrate complexes (*vide supra*). A melt reaction consists of grinding the solid ligand and metal together with a mortar and pestle, and heating the mixed-solid in the absence of solvent until it melts. When the liquid reac-

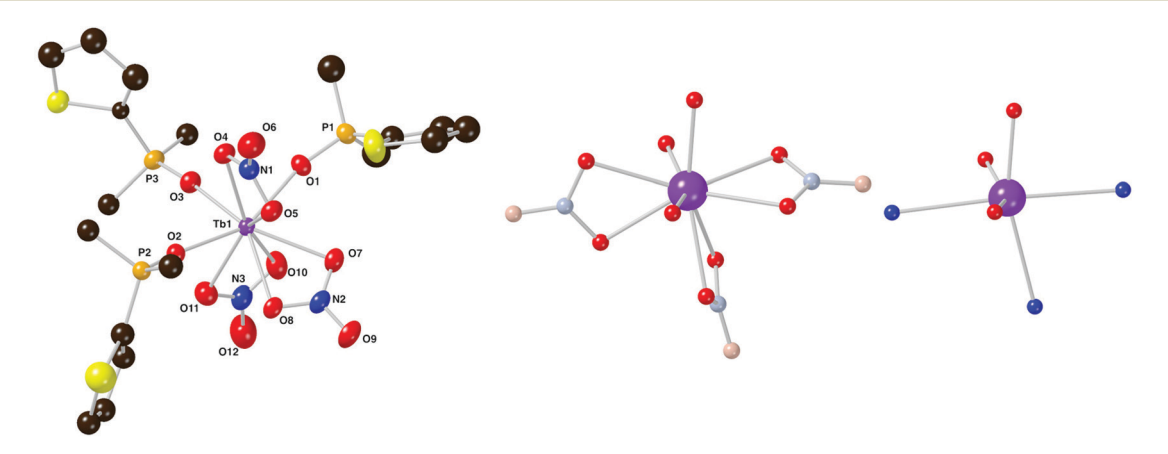


Fig. 6 Left: abbreviated X-Ray crystal structure of the $[Tb(4)_3(NO_3)_3]$ complex using CPK colors and showing the atom numbering scheme for the Tb, O, N and P atoms. All atoms except for carbon are drawn as thermal ellipsoids at the 50% probability level. Hydrogen atoms, the pendant phenyl rings of the ligand, and the benzene solvate molecule are not shown for clarity. Center: all nine oxygen atoms (red) that coordinate to the metal (nitrogen and non-coordinating oxygen atom of the nitrate groups are depicted with lighter blue and red colors); right: depiction of the bidentate nitrates as monodentate ligands through the nitrogen atom to give a six-coordinate metal (distorted octahedral geometry).

tion mixture re-solidifies, this is an indication that a compound with a higher melting point (the desired Ln-ligand complex) has been formed. The advantages of this technique are that the ligand does not need to compete with coordinating solvents such as acetonitrile for binding to the Ln center, and any waters of hydration from the metal may be boiled off during the reaction. This procedure gives a pure metal complex as a solid with no need for purification. This technique was only attempted on the thermally stable triflates, as nitrates may explosively oxidize organic fragments under the same conditions.

Analysis of the complexes by LR-MS, again introduced as dilute solutions in acetonitrile, show peaks for 1:1 or 1:2 Ln-ligand complexes. These ions were often formed by loss of two triflate anions to give dicationic species and were also adducts with CH_3CN and H_2O .

The ¹H NMR spectra of the Ln(OTf)₃ complexes (Ln = La, Sm) in CDCl₃ show slightly broadened signals in the aromatic region that are overlapping multiplets. In contrast, the ³¹P NMR spectra of these complexes contain one sharp signal that is shifted slightly downfield ($\Delta\delta$ = 5 ppm for both metals) from that of the free phosphine oxide 4. The spectra obtained here were very similar to those recorded for the nitrate complexes.

Investigation into the speciation in solution was carried out using ¹H and ³¹P NMR (CD₃CN) in a manner similar to that described for the nitrate complexes. A solution of La(OTf)₃ in CD₃CN was added incrementally to a solution of ligand 4 in

CD₃CN (Fig. 7). Again, only one set of resonances is observed in the ¹H NMR spectra of these solutions, indicating that any metal-ligand exchange process is fast on this NMR time scale. The signal in the 31P NMR shifts downfield and is broadened when large amounts of excess ligand are present (five or six equivalents), indicating that there is some free ligand in solution and that exchange is, again, intermediate on the ³¹P NMR time scale. This signal sharpens and stops shifting downfield once a 1:3 ratio of La3+ to ligand is reached, which we interpret as the absence of free ligand. Overall we draw a similar conclusion regarding the speciation of the Ln(OTf)₃-4 complexes in solutions of acetonitrile to that of the nitrate complexes: the number and geometry of the ligands surrounding the metal is fluxional at a rate that is fast on the ¹H NMR (400 MHz) time scale and that the metal likely accommodates, at most, three to four phosphine oxide ligands.

The $[Ln(4)_3(OTf)_3]$ complexes were also characterized in the solid state by IR spectroscopy and X-Ray diffraction. In the IR spectrum of the complexes, the peak corresponding to the P=O bond appears at similar wavenumbers to those reported for the $Ln(NO_3)_3$ complexes (*vide supra*).

In order to analyze the complexes with X-Ray diffraction, single crystals of the $[Tb(4)_3(OTf)_3]$ complex were grown by vapor diffusion techniques. While the solid complex was prepared as described above with a 1:3 ratio of metal to ligand, the X-Ray diffraction structure unexpectedly has a 1:4 metalligand ratio (Fig. 8). The additional ligand bound directly to

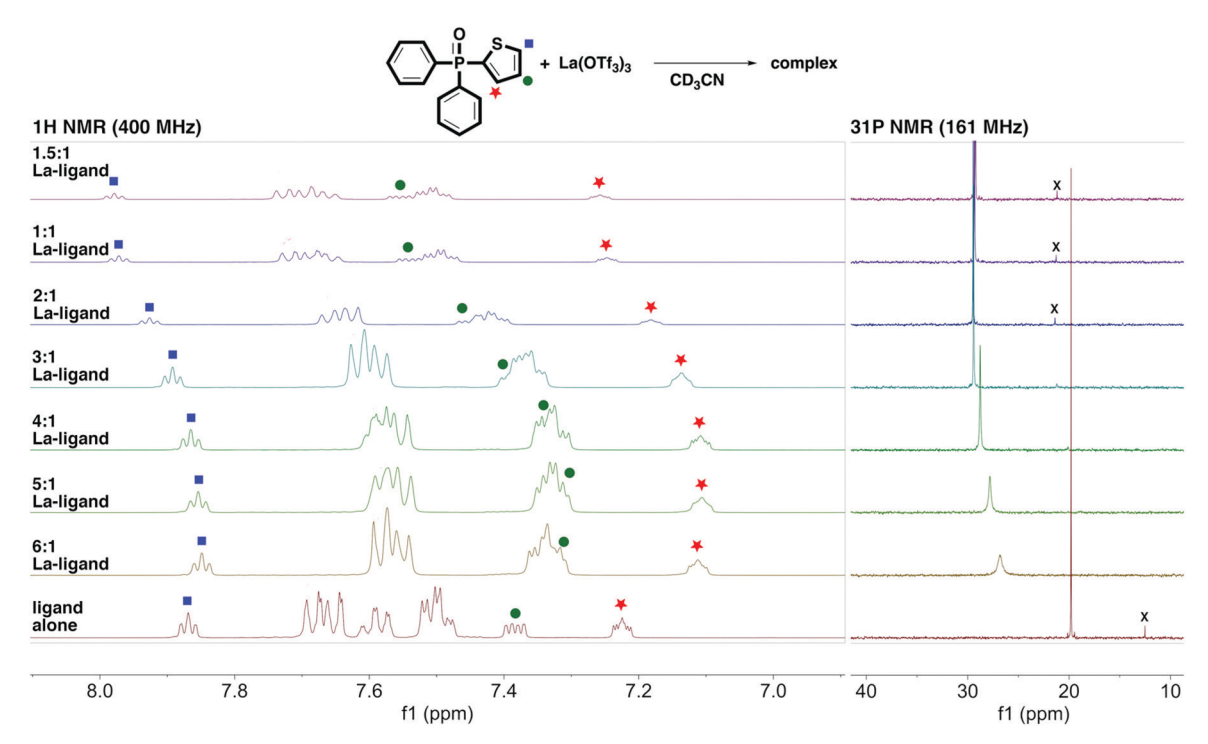


Fig. 7 NMR spectra of the titration of ligand 4 (10 mg in 0.75 mL CD₃CN) with La(OTf)₃ (1.0 M in CD₃CN) to give varying stoichiometries of metal to ligand in solution. In the ¹H NMR spectrum the resonances corresponding to the hydrogen atoms of the thienyl ring are labeled according to the diagram shown; resonances corresponding to the hydrogen atoms of the phenyl rings are unlabeled. The signal marked with a 'x' in the ³¹P NMR spectrum corresponds to a minor impurity.

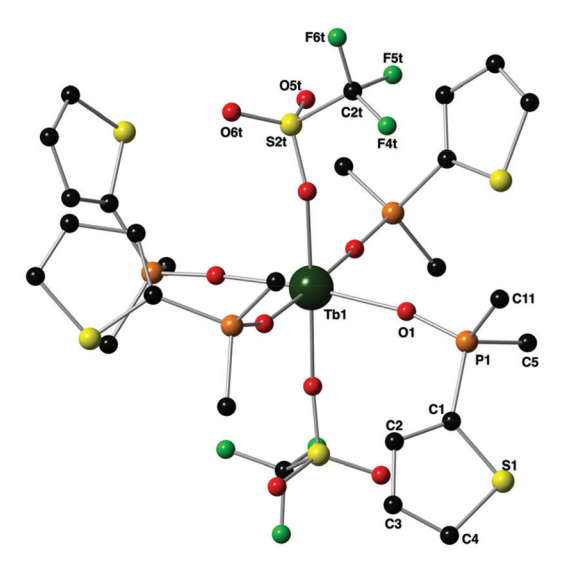


Fig. 8 Abbreviated molecular structure of $[Tb(4)_4(OTf)]_2[OTf]$ using standard CPK colors $(Tb^{3+} = dark$ green showing the atom labeling scheme one set of atoms using a ball and stick model. For clarity, only the major component is shown, while all hydrogen atoms, the pendant phenyl rings and the outer sphere triflate anion have been removed. The complete molecular structure depicting the thermal ellipsoids and labeling scheme are shown in the ESI.†

the Tb³⁺ metal comes with the expulsion of one triflate anion to the outer sphere of the complex. Our hypothesis as to why a 1:4 structure was observed here, and not with the nitrate complexes, is that triflate is a better leaving group and more easily displaced from the metal. The X-Ray crystal structure of this $[Tb(4)_4(OTf)]_2[OTf]$ complex was solved in the triclinic $P\bar{1}$ space group with the asymmetric unit containing the entire metal complex and an outer sphere triflate anion. In this structure the Tb³⁺ metal is a six-coordinate octahedron, with a square-planar arrangement of the arylphosphine oxide ligands. The apical positions of this octahedron are occupied by two triflate anions. The electron density of two of the ligand thienyl rings are again disordered and were modeled over two orientations with occupancy ratios of 67:33 and 50:50. No sulfur-pi interactions were observed for this structure. The outer sphere triflate anion and one inner sphere triflate were also disordered and were modeled over two orientations with a 50:50 occupancy ratio. The asymmetric unit also contained highly disordered electron density that was located on a symmetry site with coordinates of [0.500, 0.000, 0.000] with a volume of 176.2 Å³ and electron count of 44.5. We suspect this electron density corresponds to one molecule of toluene, and it was removed using the BYPASS procedure as executed in OLEX2.72 More details regarding the treatment of the disordered electron density in this structure can be found in the ESI.†

Selected bond lengths and angles for the [Tb $(4)_4(OTf)]_2[OTf]$ structure are listed in Table 5, and crystal data and structure refinement information can be found in Table 3. Metal-oxygen bond lengths are in the expected range, with the

Table 5 Selected bond lengths (Å) and angles (°) for [Tb(4)₄(OTf)]₂[OTf]

	$[Tb(4)_4(OTf)_2][OTf]$
Phosphine oxides	
Ln-O1(P)	2.253(3)
Ln–O2(P)	2.249(3)
Ln-O3(P)	2.228(4)
Ln–O4(P)	2.232(3)
P1-O1	1.508(4)
P2-O2	1.507(4)
P3-O3	1.507(4)
P4-O4	1.509(4)
Triflates	· · · · · · · · · · · · · · · · · · ·
Ln-O1t(S)	2.298(4)
Ln-O4t(S)	2.285(11)
Ln-O4r(S)	2.214(16)
Between ligands	. ,
O1-Ln-O2	89.51(13)
O2-Ln-O3	89.44(15)
O3-Ln-O4	88.77(15)
O4-Ln-O1	92.45(13)
O1-Ln-O1t	87.53(15)
O2-Ln-O1t	93.29(15)
O1t-Ln-O4t	177.6(5)
O1t-Ln-O4r	176.0(7)
O1-Ln-O3	173.77(13)
O2-Ln-O4	177.57(13)

Tb-O bonds from the P=O of the ligand and S=O of the triflate group being quite similar (2.21–2.30 Å). The O-Tb-O bond angles between the adjacent groups of the complex are all close to 90° (87.5–93.3°), indicating a nearly perfect octahedral arrangement of the six ligands around the metal. Considering the orientation of only the four phosphine oxide ligands around the Tb³⁺ metal, they are arranged in a nearly perfect square planar geometry with a τ_4 descriptor for four-fold coordination of 0.06 (where 1.00 = tetrahedral, 0.85 = trigonal pyramidal, 0.00 = square planar).

Summary and outlook

This paper describes a novel synthesis of diphenyl(2-thienyl) phosphine, as well as conditions to prepare the oxide, sulfide and selenide derivatives. The phosphine oxide was reacted with a series of lanthanide salts to form complexes that were characterized in solution (NMR, LR-MS) and in the solid state (IR, X-Ray diffraction). X-Ray crystallography revealed strictly nine-coordinate $[Ln(Ar_3P=O)_3(NO_3)_3]$ complexes (bidentate nitrate), with a one to three ratio between Ln and ligand. An unusually high number of these [Ln(Ar₃P=O)₃(NO₃)₃] structures gave facial-stereochemical arrangements of the six ligands, possibly attributable to sulfur-pi interactions observed in the structural data. When the counteranion is changed from nitrate to triflate, X-Ray analysis showed a strictly six-coordinate Tb-ligand complex with a one to four ratio between metal and ligand. In this complex the four ligands occupy the square planar positions of the octahedron.

As the stereochemical novelty of this work shows, explorations of non-commercially available organophosphines may be

very fertile ground for future work in related chemistry of lanthanide coordination complexes. Our future plans involve investigating the ability of the softer sulfide and selenide ligands to form complexes with actinide metals, as well as preparing the analogous phenyl(bis-2-thienyl)phosphine compound and its chalcogenide derivatives.

Conflicts of interest

There are no conflicts to declare.

Acknowledgements

We are grateful to the National Science Foundation for student (REU CHE-1559886; T. Luster, A. Spyker; K. Korman) and instrument (MRI CHE-1725669, 400 MHz JEOL NMR; MRI CHE-1919817, Advion UPLC-MS; CCLI CHE-0087655, 300 MHz JEOL NMR) financial support. We also thank GVSU for funding (chemistry department Weldon Fund, CSCE) and GVSU OURS for a S3 fellowship to G. Sands. The CCD-based X-ray diffractometers at MSU were purchased/upgraded using department funds, and we thank the National Science Foundation for support to purchase the Rigaku Synergy S. Diffractometer (MRI CHE-1919565). Finally, we thank Horst Puschman (Olex2) for help building the model for the [La $(4)_3(NO_3)_3$ structure.

References

- 1 S. Cotton, Lanthanide and Actinide Chemistry, Wiley, 2006, pp. 280.
- 2 J.-C. G. Bünzli, Eur. J. Inorg. Chem., 2017, 5058-5063.
- 3 J.-C. G. Bünzli, J. Lumin., 2016, 170, 866-878.
- 4 M. C. Heffern, L. M. Matosziuk and T. J. Meade, Chem. Rev., 2014, 114, 4496-4539.
- 5 Z. Zhu, M. Guo, X.-L. Li and J. Tang, Coord. Chem. Rev., 2019, 378, 350-364.
- 6 A. de Bettencourt-Dias, in Luminescence of Lanthanide Ions in Coordination Compounds and Nanomaterials, Wiley, Chichester, 1st edn, 2014, pp. 384.
- 7 S. V. Eliseeva and J.-C. G. Bünzli, Chem. Soc. Rev., 2010, 39, 189-227.
- 8 S. SeethaLekshmi, A. R. Ramya, M. L. P. Reddy and S. Varughese, J. Photochem. Rev., 2017, 33, 109-131.
- 9 N. Tsoulfanidis, The Nuclear Fuel Cycle, American Nuclear Society, La Grange Park, 2013, pp. 478.
- 10 J. Lux and A. D. Sherry, Curr. Opin. Chem. Biol., 2018, 45, 121-130.
- 11 U.S. Department of Energy, Critical Minerals and Materials, Washington, DC, 2021, pp. 1-50.
- 12 "Critical Minerals & Materials: Chemical and Materials Sciences Research on Rare Earth and Platinum Group Elements" US Department of Energy, Office of Science, Basic Energy Sciences; FOA DE-FOA-0002483.

13 J. P. Collman, L. S. Hegedus, J. R. Norton and R. G. Finke, Principles and applications of organotransition metal chemistry. 1st ed, Univ. Science Books, 1987.

- 14 F. A. Cotton, G. Wilkinson, C. A. Murillo and M. Bochmann, Advanced Inorganic Chemistry, John Wiley & Sons, Inc., Chichester, 6th edn, 1999.
- 15 A. Bowden, P. N. Horton and A. W. G. Platt, Inorg. Chem., 2011, 50, 2533-2561.
- 16 A. W. G. Platt, Coord. Chem. Rev., 2017, 340, 62-78.
- 17 A. Bowden, A. W. G. Platt, K. Singh and R. Townsend, Inorg. Chim. Acta, 2010, 363, 243-249.
- 18 J.-C. Berthet, M. Nierlich and M. Ephritikhine, Angew. Chem., Int. Ed., 2003, 42, 1952-1954.
- 19 J.-C. Berthet, M. Nierlich and M. Ephritikhine, Polyhedron, 2003, 22, 3475-3482.
- 20 M. J. Glazier, W. Levason, M. L. Matthews, P. L. Thornton and M. Webster, *Inorg. Chim. Acta*, 2004, 357, 1083–1091.
- 21 N. J. Hill, L.-S. Leung, W. Levason and M. Webster, Inorg. Chim. Acta, 2003, 343, 169-174.
- 22 A. C. Behrle, C. L. Barnes, N. Kaltsoyannis and J. R. Walensky, Inorg. Chem., 2013, 52, 10623-10631.
- 23 COSMO v1.61 Software for the CCD detector systems for determining data collection parameters, Bruker Analytical X-ray Systems, Madison, WI, 2009.
- 24 CrysAlisPro, Rigaku, V1.171.40.84a, 2020.
- 25 APEX2 v2010.11-3 Software for the CCD detector system, Bruker Analytical X-ray Systems, Madison, WI, 2010.
- 26 SAINT v7.68A Software for the Integration of CCD Detector System, Bruker Analytical X-ray Systems, Madison, WI, 2010.
- 27 R. H. Blessing, Acta Crystallogr., Sect. A: Found. Crystallogr., 1995, 51, 33-38.
- 28 G. M. Sheldrick, Acta Crystallogr., Sect. A: Found. Crystallogr., 2008, 64, 112-122.
- 29 O. V. Dolomanov, L. J. Bourhis, R. J. Gildea, J. A. K. Howard and H. Puschmann, J. Appl. Crystallogr., 2009, 42, 339-341.
- 30 L. J. Bourhis, O. V. Dolomanov, R. J. Gildea, J. A. K. Howard and H. Puschmann, Acta Crystallogr., Sect. A: Found. Adv, 2015, 71, 59-75.
- 31 J. Xu, P. Zhang, Y. Gao, Y. Chen, G. Tang and Y. Zhao, J. Org. Chem., 2013, 78, 8176-8183.
- 32 M. Bosson, W. Levason, T. Patel, M. C. Popham and M. Webster, *Polyhedron*, 2001, **20**, 2055–2062.
- 33 D. Allen, J. R. Charlton and B. G. Hutley, Phosphorus Relat. Group V Elem., 1976, 6, 191-194.
- 34 A. J. Deeming, S. N. Jayasuriya, A. J. Arce and Y. De Sanctis, Organometallics, 1996, 15, 786-793.
- 35 K. Isslieb and F. Z. Krech, Z. Anorg. Allg. Chem., 1964, 328, 21-33.
- 36 J. Lloret, K. Bieger, F. Estevan, P. Lahuerta, P. Hirva, J. Pérez-Prieto and M. Sanaú, Organometallics, 2006, 25, 5113-5121.
- 37 D. Cauzzi, C. Graiff, C. Massera, G. Predieri and A. Tiripicchio, J. Cluster Sci., 2001, 12, 259–271.
- 38 A. J. Deeming, M. K. Shinhmar, A. J. Arce and Y. De Sanctis, J. Chem. Soc., Dalton Trans., 1999, 1153-1160.

- 39 L. Horner and J. Roder, *Phosphorus*, 1976, 6, 147-150.
- 40 N. Nowrouzi, S. Keshtgar and E. B. Jahromi, *Tetrahedron Lett.*, 2015, 57, 348–350.
- 41 F. Y. Kwong, C. W. Lai, M. Yu and K. S. Chan, *Tetrahedron*, 2004, **60**, 5635–5645.
- 42 S. E. Tunney and J. K. Stille, J. Org. Chem., 1987, 52, 748-753.
- 43 D. Van Allen and D. Venkataraman, *J. Org. Chem.*, 2003, **68**, 4590–4593.
- 44 E. R. Clark, A. M. Borys and K. Pearce, *Dalton Trans.*, 2016, 16125–16129.
- 45 K. N. Brown and J. H. Espenson, *Inorg. Chem.*, 1996, 35, 7211–7216.
- 46 J. Nakayama, H. Nagasawa, Y. Sugihara and A. Ishii, *J. Am. Chem. Soc.*, 1997, **119**, 9077–9078.
- 47 T. Thiemann, D. J. Walton, A. O. Brett, J. Iniesta, F. Marken and Y.-q. Li, In 5th Eurasian Conference on Heterocyclic Chemistry, 2009, pp 96–113.
- 48 S. Wang, Q. Xue, Z. Guan, Y. Ye and A. Lei, *ACS Catal.*, 2021, 11, 4295–4300.
- 49 T. Wang, S. Sang, L. L. Liu, H. Qiao, Y. Gao and Y. Zhao, *J. Org. Chem.*, 2013, **79**, 608–617.
- 50 Y. Bai, N. Liu, S. Wang, S. Wang, S. Ning, L. Shi, L. Cui, Z. Zhang and J. Ziang, *Org. Lett.*, 2019, 21, 6835–6838.
- 51 R. Henyecz, R. Oroszy and G. Keglevich, *Curr. Org. Chem.*, 2019, 23, 1151–1157.
- 52 M. B. Kurosawa, R. Isshiki, K. Muto and J. Yamaguchi, *J. Am. Chem. Soc.*, 2020, **142**, 7386–7392.
- 53 M. Koohgard, H. Karimitabar and M. Hosseini-Sarvari, *Dalton Trans.*, 2020, **49**, 17147–17151.
- 54 Z. Chen, X. Liu, H. Zhu and Z. Wang, *Tetrahedron*, 2021, **81**, 131912.
- 55 R. Isshiki, K. Muto and J. Yamaguchi, *Org. Lett.*, 2018, **20**, 1150–1153.

- 56 F. J. Arnáiz and R. Aguado, J. Chem. Educ., 1995, 72, A196– A198.
- 57 R. A. Zingaro and E. A. Meyers, *Inorg. Chem.*, 1962, 1, 771.
- 58 C. Screttas and A. F. Isbell, J. Org. Chem., 1962, 27, 2573.
- 59 P. Nicpon and D. W. Meek, *Inorg. Chem.*, 1966, 5, 1297.
- 60 S. O. Grim and E. D. Walton, *Phosphorus, Sulfur Silicon Relat. Elem.*, 1980, 9, 123.
- 61 L. Yang, D. R. Powell and R. P. Houser, *Dalton Trans.*, 2007, 955–964.
- 62 MestReNova, version 12.0.3-21384 (https://www.mestrelab.com).
- 63 A. Ruiz-Martínez, D. Casanova and S. Alvarez, *Dalton Trans.*, 2008, 2583–2591.
- 64 D. Casanova, J. Cirera, M. Llunell, P. Alemany, D. Avnir and S. Alvarez, *J. Am. Chem. Soc.*, 2004, **126**, 1755–1763.
- 65 J. Hwang, P. Li, M. D. Smith, C. E. Warden, D. A. Sirianni, E. C. Vik, J. M. Maier, C. J. Yehl, C. D. Sherrill and K. D. Shimizu, *J. Am. Chem. Soc.*, 2018, **140**, 13301–13307.
- 66 E. A. Meyer, R. K. Castellano and F. Diederich, *Angew. Chem., Int. Ed.*, 2003, **42**, 1210–1250.
- 67 Y. Ma, S. Xu, X. Wang, M. Liu, Y.-X. Li, X.-L. Xin and Q.-H. Jin, *Z. Anorg. Allg. Chem.*, 2017, **643**, 780–788.
- 68 A. P. Hunter, A. M. J. Lees and A. W. G. Platt, *Polyhedron*, 2007, 26, 4865–4876.
- 69 A. Bowden, P. N. Horton and A. W. G. Platt, *Inorg. Chem.*, 2011, **50**, 2553–2561.
- 70 A. Bowden, S. J. Coles, M. B. Pitak and A. W. G. Platt, Polyhedron, 2014, 68, 258–264.
- 71 W. Levason, E. H. Newman and M. Webster, *Polyhedron*, 2000, 2697–2705.
- 72 P. van der Sluis and A. L. Spek, *Acta Crystallogr., Sect. A: Found. Crystallogr.*, 1990, **46**, 194–201.